Ash1l controls quiescence and self-renewal potential in hematopoietic stem cells

Morgan Jones,[1,2,3] Jennifer Chase,[1,2] Michelle Brinkmeier,[4] Jing Xu,[5] Daniel N. Weinberg,[1] Julien Schira,[1] Ann Friedman,[1] Sami Malek,[6] Jolanta Grembecka,[5] Tomasz Cierpicki,[5] Yali Dou,[5] Sally A. Camper,[4] and Ivan Maillard[1,6,7]

[1]Center for Stem Cell Biology, Life Sciences Institute, [2]Graduate Program in Cellular and Molecular Biology, [3]Medical Scientist Training Program, [4]Department of Human Genetics, [5]Department of Pathology, [6]Division of Hematology-Oncology, Department of Internal Medicine, and [7]Department of Cell and Developmental Biology, University of Michigan, Ann Arbor, Michigan, USA.

Rapidly cycling fetal and neonatal hematopoietic stem cells (HSCs) generate a pool of quiescent adult HSCs after establishing hematopoiesis in the bone marrow. We report an essential role for the trithorax group gene absent, small, or homeotic 1-like (*Ash1l*) at this developmental transition. Emergence and expansion of *Ash1l*-deficient fetal/neonatal HSCs were preserved; however, in young adult animals, HSCs were profoundly depleted. *Ash1l*-deficient adult HSCs had markedly decreased quiescence and reduced cyclin-dependent kinase inhibitor 1b/c (*Cdkn1b/1c*) expression and failed to establish long-term trilineage bone marrow hematopoiesis after transplantation to irradiated recipients. Wild-type HSCs could efficiently engraft when transferred to unirradiated, *Ash1l*-deficient recipients, indicating increased availability of functional HSC niches in these mice. *Ash1l* deficiency also decreased expression of multiple Hox genes in hematopoietic progenitors. *Ash1l* cooperated functionally with mixed-lineage leukemia 1 (*Mll1*), as combined loss of *Ash1l* and *Mll1*, but not isolated *Ash1l* or *Mll1* deficiency, induced overt hematopoietic failure. Our results uncover a trithorax group gene network that controls quiescence, niche occupancy, and self-renewal potential in adult HSCs.

Introduction

Fetal hematopoietic stem cells (HSCs) proliferate rapidly and contribute to massive expansion of the HSC pool (1, 2). In contrast, adult HSCs divide rarely in steady-state conditions, as a majority of cells reside in the quiescent G_0 phase of the cell cycle and return to quiescence after periods of proliferation (3–8). In mice, transition from the fetal/neonatal to the adult HSC program occurs in the bone marrow (BM) niche within weeks after birth and coincides with establishment of HSC quiescence, functional and phenotypic changes, and downregulated expression of the transcription factor *Sox17* and other fetal HSC genes (1, 9–12). Failure to establish or maintain quiescence has been linked to adult HSC depletion, increased sensitivity to myeloablation, and reduced engraftment in transplantation assays (1, 13–16). However, the regulatory mechanisms controlling quiescence and successful initiation of the adult HSC program in the BM remain poorly understood.

The trithorax group (TrxG) is a diverse family of epigenetic regulators originally identified to control body patterning in *Drosophila* (17). In flies, individual TrxG members cooperate to promote expression of homeobox (Hox) genes, and combined heterozygous TrxG gene mutations act as dominant enhancers of one another (18, 19). Mixed-lineage leukemia 1 (*Mll1*) is the trithorax homolog and founding TrxG member in mammals. In humans, *MLL1* was first identified as a recurrent translocation partner in acute leukemias characterized by upregulated HOX gene expression (20–23). Endogenous *Mll1* regulates expression of Hox genes and other targets as well as the function of normal HSCs (24–26). *Mll1* encodes a large protein containing a C-terminal Su(var)3-9/enhancer-of-zeste/trithorax (SET) domain with H3K4 histone methyltransferase activity (27). MLL1 functions as a part of a multiprotein complex that includes RBBP5, WDR5, and ASH2L (28–31). Limited information is available about cooperative interactions among mammalian TrxG members, in particular with proteins in which an association with the MLL complex has not been as yet identified.

The TrxG gene absent, small, or homeotic 1 (*ash1*) was first discovered in genetic screens seeking regulators of *Drosophila* imaginal discs (32). *ash1* encodes a large protein containing an internal SET domain with putative histone methyltransferase activity (33). Its mammalian homolog *Ash1l* also encodes a SET domain–containing protein that can associate with actively transcribed loci, including at several Hox genes (34–36). However, unlike the much smaller protein ASH2L, ASH1L has not been identified so far as a member of the MLL protein complex. Recently, the ASH1L SET domain was reported to have intrinsic H3K36 dimethyltransferase activity using in vitro biochemical assays (37–39). Neither the physiological significance of *Ash1l* nor the idea of cooperativity with *Mll1* and other TrxG members has been evaluated in vivo.

In this report, we describe an essential role for the TrxG member *Ash1l* in the maintenance and function of adult HSCs but not in the in vivo expansion of fetal or neonatal hematopoietic progenitors. *Ash1l* was essential for the establishment of quiescence at the fetal to adult HSC transition in the BM within weeks after birth. *Ash1l* deficiency led to profound depletion of adult HSCs and multipotent progenitors as well as to a lack of functional HSCs capable of long-term BM reconstitution in transplantation assays. Unlike

Authorship note: Morgan Jones and Jennifer Chase contributed equally to this work.
Conflict of interest: The authors have declared that no conflict of interest exists.
Submitted: July 21, 2014; **Accepted:** March 12, 2015.
Reference information: *J Clin Invest*. 2015;125(5):2007–2020. doi:10.1172/JCI78124.

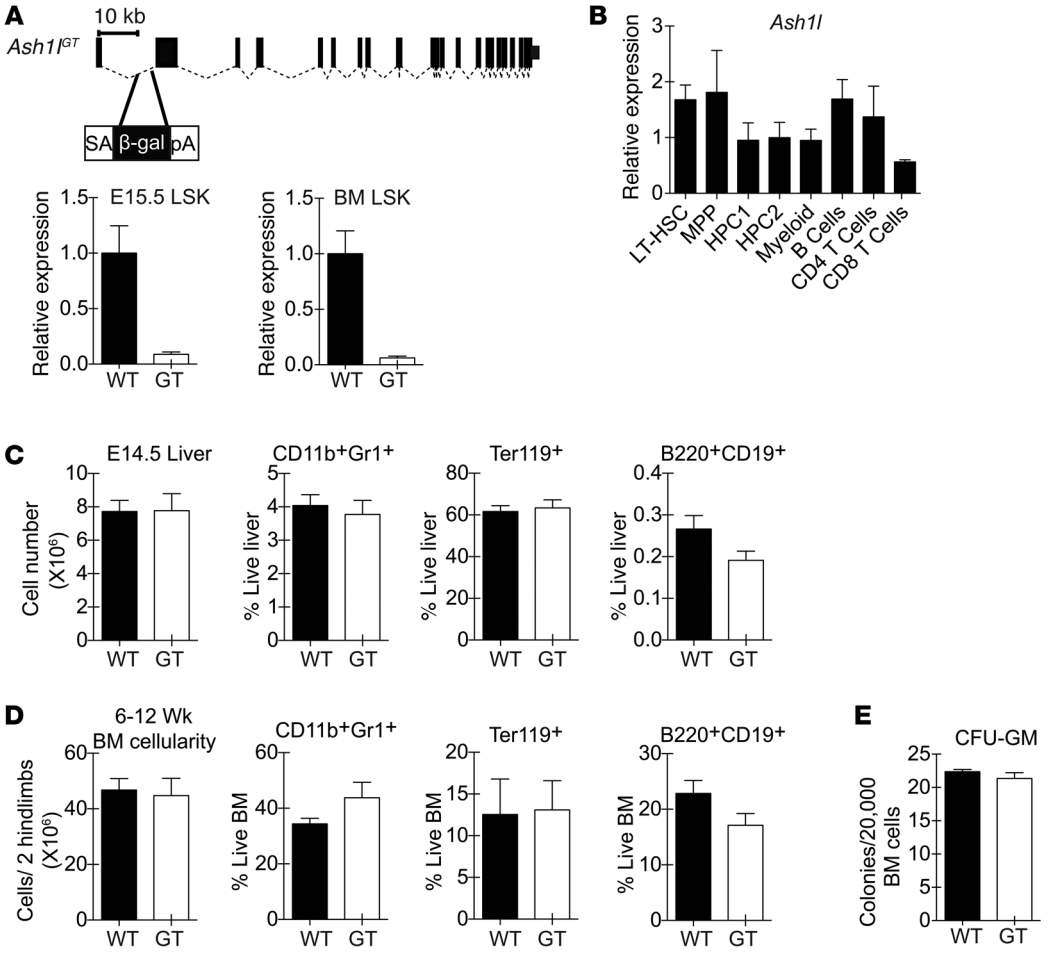

Figure 1. Preserved overall fetal and adult hematopoietic output in *Ash1l*$^{GT/GT}$ mice. (**A**) Generation of the *Ash1l*^{GT} allele by insertion of a splice-acceptor gene trap cassette into the first *Ash1l* intron. Homozygosity led to >90% reduction in wild-type transcripts in fetal (E15.5) and adult LSK progenitors, as shown by quantitative RT-PCR (qRT-PCR) with primers amplifying cDNA across the exon 1–2 boundary (mean ± SD). (**B**) qRT-PCR analysis of *Ash1l* expression normalized to *Hprt1* in selected hematopoietic populations (LT-HSC, LSK CD150$^+$CD48$^-$ LT-HSCs; MPP, LSK MPPs; HPC1, LSK CD150$^-$CD48$^+$ hematopoietic progenitor cells; HPC2, LSK CD150$^+$CD48$^+$ hematopoietic progenitor cells; myeloid, CD11b$^+$Gr1$^+$ myeloid cells; B cells, B220$^+$AA4.1$^-$ B cells; CD4 T cells, TCRβ$^+$CD4$^+$ cells; CD8 T cells, TCRβ$^+$CD8$^+$ T cells) (mean ± SD). (**C**) Cellularity and percentage of myeloid, erythroid, and B lineage cells in E14.5 wild-type and *Ash1l*$^{GT/GT}$ (GT) fetal liver ($n \geq 4$ per genotype from 2 independent experiments; mean ± SEM). (**D**) Cellularity and percentage of myeloid, erythroid, and B lineage cells in young adult (6- to 12-week-old) wild-type and *Ash1l*$^{GT/GT}$ BM ($n \geq 6$ per genotype from >2 independent experiments; mean ± SEM). (**E**) Myeloid colony formation by wild-type and *Ash1l*$^{GT/GT}$ BM in CFU-GM assays (mean ± SEM, representative of 2 experiments). No statistically significant differences by *t* test.

in wild-type recipients, after nonmyeloablative transplantation of normal HSCs, cells could efficiently engraft the BM and establish durable hematopoiesis in *Ash1l*-deficient mice, suggesting poor competition of residual HSCs for niche space. Despite profound defects in transplantation assays, *Ash1l*-deficient mice exhibited no overt hematopoietic failure in steady-state conditions, with evidence of increased self-renewal in progenitors downstream of HSCs. However, combining *Ash1l* deficiency with inactivation of the TrxG gene *Mll1* or its cofactor gene *Men1* led to rapid BM failure. These data reveal an essential physiological function for the TrxG gene *Ash1l* in adult HSCs and represent the first genetic demonstration of cooperativity between TrxG members in mammals.

Results

Ash1l-deficient mice have normal numbers of fetal and neonatal HSCs but profound depletion of adult HSCs. To examine the function of *Ash1l* in hematopoiesis, we used a gene trap insertion allele containing a splice-acceptor cassette in the first *Ash1l* intron (Figure 1A). This strategy resulted in a >90% reduction of full-length *Ash1l* transcripts in fetal liver and BM lineage$^-$SCA1$^+$c-KIT$^+$ (LSK) HSCs and hematopoietic progenitor cells. *Ash1l* was expressed in all subpopulations of LSK progenitors and in selected mature cell subsets (Figure 1B). Homozygosity for the *Ash1l*^{GT} allele preserved fetal liver and BM cellularity as well as myeloid, erythroid, and B lineage cells in *Ash1l*$^{GT/GT}$ mice compared with that in *Ashl*$^{+/+}$ littermates (Figure 1, C and D). The capacity to form myeloid colonies was normal in *Ash1l*-deficient BM, consistent with preserved progenitor numbers and function (Figure 1E).

We quantified HSCs as the CD150$^+$CD48$^-$ fraction of LSK progenitors, a definition that identifies both fetal and adult long-term HSCs (LT-HSCs) (40, 41). *Ash1l*-deficient LT-HSCs were present at normal frequency in the fetal liver, showing that phenotypically defined fetal LT-HSCs emerged and expanded normally in these mice (Figure 2A). HSC numbers were also preserved in the

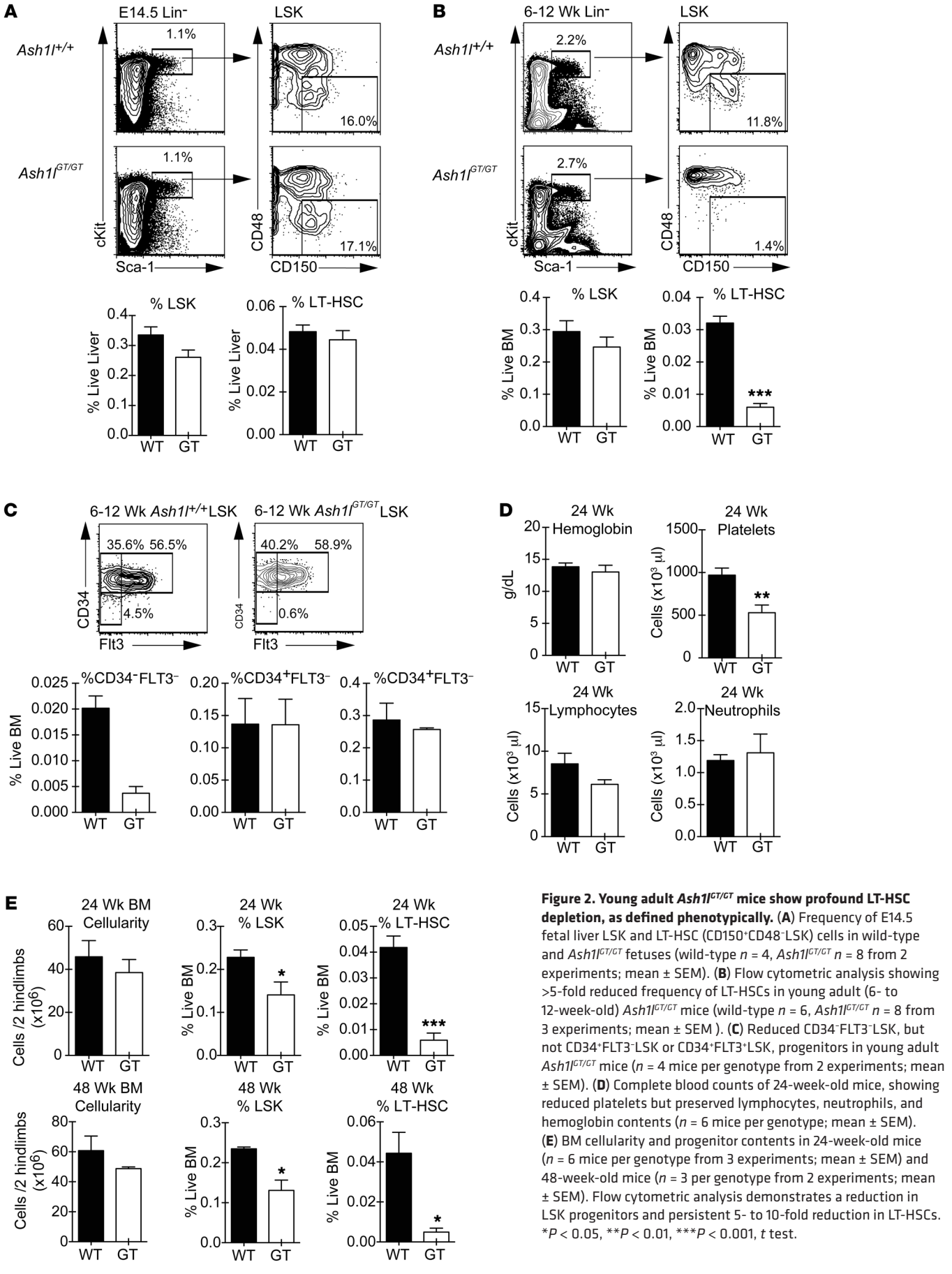

Figure 2. Young adult *Ash1l*$^{GT/GT}$ mice show profound LT-HSC depletion, as defined phenotypically. (**A**) Frequency of E14.5 fetal liver LSK and LT-HSC ($CD150^+CD48^-$LSK) cells in wild-type and *Ash1l*$^{GT/GT}$ fetuses (wild-type $n = 4$, *Ash1l*$^{GT/GT}$ $n = 8$ from 2 experiments; mean ± SEM). (**B**) Flow cytometric analysis showing >5-fold reduced frequency of LT-HSCs in young adult (6- to 12-week-old) *Ash1l*$^{GT/GT}$ mice (wild-type $n = 6$, *Ash1l*$^{GT/GT}$ $n = 8$ from 3 experiments; mean ± SEM). (**C**) Reduced $CD34^-FLT3^-$LSK, but not $CD34^+FLT3^-$LSK or $CD34^+FLT3^+$LSK, progenitors in young adult *Ash1l*$^{GT/GT}$ mice ($n = 4$ mice per genotype from 2 experiments; mean ± SEM). (**D**) Complete blood counts of 24-week-old mice, showing reduced platelets but preserved lymphocytes, neutrophils, and hemoglobin contents ($n = 6$ mice per genotype; mean ± SEM). (**E**) BM cellularity and progenitor contents in 24-week-old mice ($n = 6$ mice per genotype from 3 experiments; mean ± SEM) and 48-week-old mice ($n = 3$ per genotype from 2 experiments; mean ± SEM). Flow cytometric analysis demonstrates a reduction in LSK progenitors and persistent 5- to 10-fold reduction in LT-HSCs. $^*P < 0.05$, $^{**}P < 0.01$, $^{***}P < 0.001$, *t* test.

neonatal liver (data not shown). However, by 6 to 12 weeks after birth, LT-HSCs had decreased by 5- to 10-fold in *Ash1l*$^{GT/GT}$ BM as compared with BM of wild-type littermates (Figure 2B). A similar profound reduction was observed using the CD34$^-$FLT3$^-$LSK phenotype as an alternative definition of LT-HSCs, with preserved frequencies of CD34$^+$FLT3$^-$ and CD34$^+$FLT3$^+$ downstream progenitors (Figure 2C and refs. 42, 43). We next fractionated LSK progenitors using CD150/CD48 expression, as the functional potential of these subpopulations was recently characterized in detail (44). Both LSK CD150$^+$CD48$^-$ LT-HSCs and CD150$^-$CD48$^-$ multipotent progenitors (MPPs), but not CD48$^+$LSK hematopoietic progenitor cells (HPC1/2), were decreased in *Ash1l*$^{GT/GT}$ mice (Supplemental Figure 1; supplemental material available online with this article; doi:10.1172/JCI78124DS1). Despite persistent LT-HSC depletion, 24-week-old *Ash1l*-deficient mice maintained normal blood counts, except for modest thrombocytopenia (Figure 2D). Overall BM cellularity remained preserved at 24 weeks as well as at 48 weeks of life. Flow cytometric analysis showed persistent profound LT-HSC depletion, while numbers of LSK progenitors were reduced only by about 30% at 24 weeks and 50% at 48 weeks (Figure 2E). These data suggest a specific role of *Ash1l* in the maintenance of adult BM HSCs, with downstream compensatory mechanisms preserving overall hematopoietic function in steady-state conditions.

To evaluate whether the hematopoietic phenotype of *Ash1l*-deficient mice was associated with mobilization of BM HSCs and hematopoietic progenitor cells into the periphery, we assessed LSK and LT-HSC frequency as well as colony-forming activity in the spleen (Supplemental Figure 2). The frequency of spleen LSK/LT-HSCs and granulocyte-macrophage CFU (CFU-GM) colonies was decreased in *Ash1l*$^{GT/GT}$ mice. These findings indicate the absence of a mobilization phenotype in these mice and suggest that the maintenance of adult *Ash1l*-deficient hematopoietic progenitors was relatively more impaired outside as compared with that within the BM.

Ash1l-deficient mice lack HSCs capable of long-term BM reconstitution after transplantation. As the gold standard definition of LT-HSCs is based on their function (45, 46), we studied the long-term reconstitution potential of *Ash1l*-deficient progenitors in transplantation assays (Figure 3A). This strategy allowed us to evaluate LT-HSC function irrespective of surface phenotype. We transplanted lethally irradiated CD45.1$^+$ recipient mice with CD45.2$^+$ *Ash1l*$^{GT/GT}$ or *Ash1l*$^{+/+}$ BM and an equal number of CD45.1$^+$ competitor BM cells. Although transient output was observed 2 weeks after transplantation, *Ash1l*$^{GT/GT}$ BM failed to support long-term trilineage reconstitution of the myeloid, B, and T cell compartments (Figure 3B). Analysis of BM LT-HSCs 10–16 weeks after transplantation showed a complete absence of *Ash1l*$^{GT/GT}$ LT-HSCs (Figure 3, C and D). The lack of significant reconstitution beyond a few weeks was consistent with the depletion of both LT-HSCs and multipotent progenitors in *Ash1l*-deficient mice, as defined using CD150/CD48 expression (43). To examine the relative contribution of CD48$^-$LSK cells (containing LT-HSCs and multipotent progenitors) and CD48$^+$LSK cells (containing HPC1/2 progenitors) to transient reconstitution after transplant, we competitively transferred sort-purified CD48$^-$LSK and CD48$^+$LSK progenitors to lethally irradiated recipients (Supplemental Figure 3). Consistent with past data (44), only transient hematopoietic output was detected from wild-type HPC1/2 cells, while LSK MPP/LT-HSC sustained long-term reconstitution. This pattern of activity was preserved with *Ash1l*-deficient progenitors at early time points after transplantation, with the bulk of short-term reconstitution coming from the CD48$^-$LSK fraction (2–4 weeks after transplant). As observed with transplantation of total BM, however, phenotypically defined MPP/LT-HSCs were functionally unable to sustain long-term reconstitution. These data suggest that *Ash1l*-deficient CD48$^-$LSK cells can home to the BM and provide initial progeny but lack long-term self-renewal potential.

We next examined *Ash1l*$^{GT/GT}$ LT-HSC function after transplantation without competition. The majority of irradiated *Ash1l*$^{GT/GT}$ BM recipients died within 10 to 150 days after transplantation, consistent with transient radioprotection but suggestive of LT-HSC dysfunction (Figure 3E). Surviving *Ash1l*$^{GT/GT}$ BM recipients exhibited host CD45.1$^+$ reconstitution and no *Ash1l*$^{GT/GT}$ LT-HSCs (Figure 3F). Thus, *Ash1l*$^{GT/GT}$ BM did not house transplantable LT-HSCs, even as defined by noncompetitive transplantation.

We then performed transplantation using fetal liver as the donor source, thereby normalizing phenotypic LT-HSC frequency and eliminating the possibility that stromal BM defects contributed to LT-HSC dysfunction (Figure 4A). *Ash1l*$^{GT/GT}$ fetal liver progenitors were incapable of sustaining myeloid, B, and T lineage reconstitution after transplantation (Figure 4B). Analysis of the BM at 17 to 26 weeks after transplantation showed no detectable *Ash1l*$^{GT/GT}$ LT-HSCs (Figure 4C). Thus, fetal *Ash1l*$^{GT/GT}$ LT-HSCs were present in normal numbers, as defined phenotypically, but could not establish durable hematopoiesis in the BM after transplantation, indicating that they were functionally defective once transferred into the postnatal environment.

To evaluate the homing capacity of *Ash1l*-deficient progenitors, we analyzed recipient BM 24 hours after transplantation into nonirradiated mice (Supplemental Figure 4A). Equivalent numbers of donor-derived wild-type and *Ash1l*$^{GT/GT}$ cells were recovered (Supplemental Figure 4B). Similar observations were made in irradiated recipients (data not shown). Altogether, our findings reveal profound LT-HSC dysfunction that becomes apparent in the context of the adult BM niche after transplantation, despite preserved initial homing and even when fetal cells are used as a source of progenitors.

The Ash1l-deficient BM supports wild-type HSC engraftment in the absence of myeloablation. Since *Ash1l*$^{GT/GT}$ BM had reduced LT-HSCs that were nonfunctional in transplantation assays, we reasoned that available niche space and/or defective progenitors could allow engraftment of donor HSCs without myeloablation. We infused 2 boluses of wild-type CD45.1$^+$ BM (or *B6-GFP* BM in selected experiments) into CD45.2$^+$ *Ash1l*$^{+/+}$ or *Ash1l*$^{GT/GT}$ mice without prior irradiation (Figure 5A). Few, if any, donor-derived cells engrafted in wild-type recipients, as expected. In contrast, the majority (7 of 8) of *Ash1l*$^{GT/GT}$ recipients achieved stable or steadily rising trilineage output from infused BM, as shown by the 20% to 90% donor-derived contribution to blood lineages for ≥12 weeks (Figure 5B). At completion of the experiment, donor LT-HSCs were present in the *Ash1l*$^{GT/GT}$ BM (Figure 5C). Thus, the *Ash1l*$^{GT/GT}$ BM niche supported long-term stable engraftment by wild-type HSCs, while residual *Ash1l*$^{GT/GT}$ HSCs and hematopoietic progenitor cells competed poorly for niche space.

Neonatal Ash1l$^{GT/GT}$ *HSCs home to the BM but fail to establish a quiescent adult HSC pool*. As LT-HSC loss was first observed in young adult *Ash1l*$^{GT/GT}$ BM, we studied BM HSCs within 1 to 3 weeks after

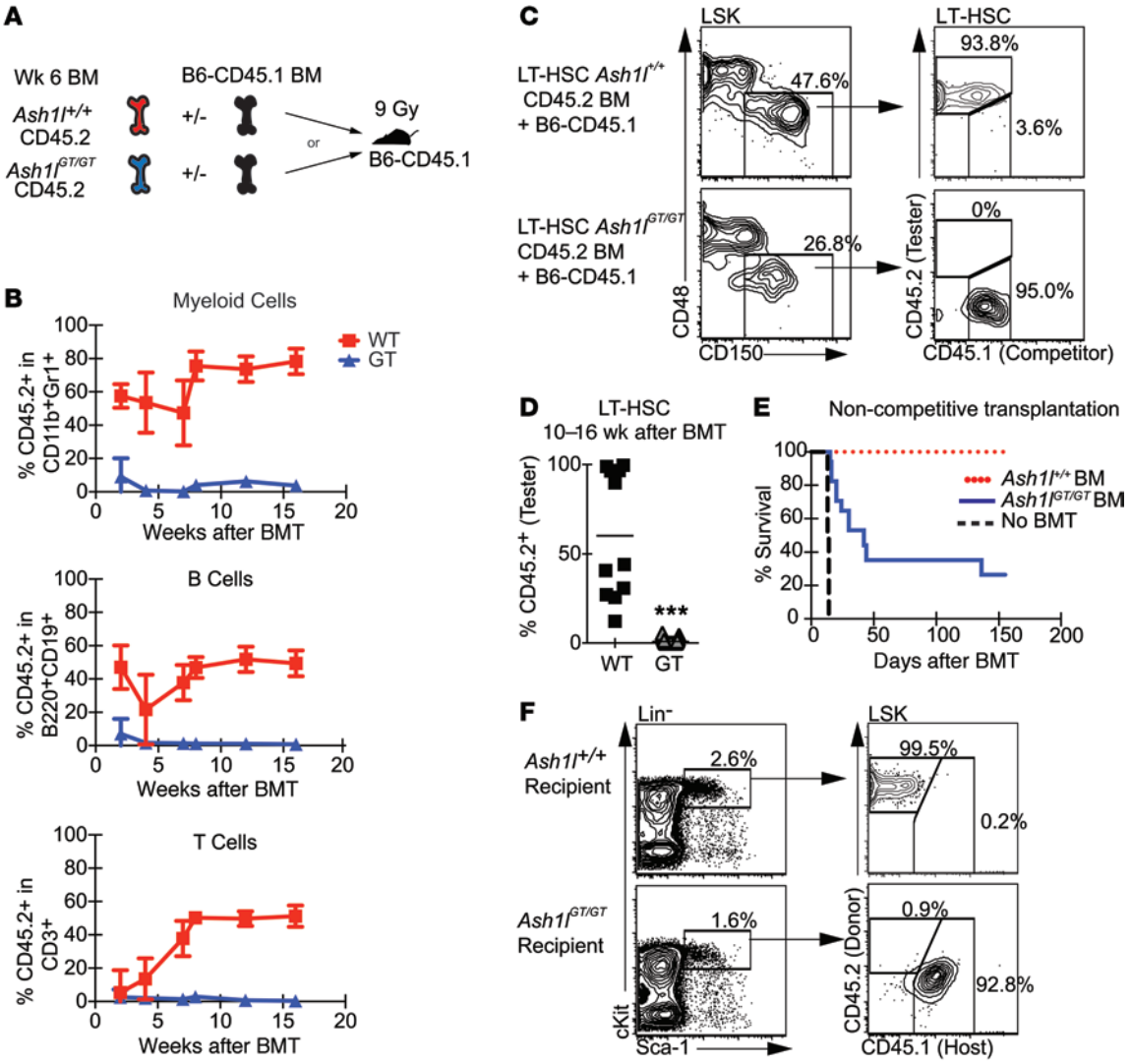

Figure 3. Competitive and noncompetitive transplantation assays reveal a lack of *Ash1l*-deficient HSCs capable of long-term hematopoietic reconstitution. (**A**) Experimental strategy: *Ash1l*$^{+/+}$or *Ash1l*$^{GT/GT}$ B6-CD45.2 BM was injected into irradiated (9 Gy) B6-CD45.1 recipients, with or without B6-CD45.1 competitor BM (5×10^5 cells each for competitive transplantation and 10^6 cells for noncompetitive transplantation). (**B**) Peripheral blood analysis 2–16 weeks after competitive transplantation, showing a profound reduction of *Ash1l*$^{GT/GT}$ BM contribution to myeloid, B, and T lineage reconstitution (wild-type $n = 11$, *Ash1l*$^{GT/GT}$ $n = 23$; mean ± SD from 2 experiments). BMT, BM transplantation. (**C** and **D**) CD45.2/CD45.1 chimerism in BM LT-HSCs 10–16 weeks after transplantation, showing absence of *Ash1l*$^{GT/GT}$ LT-HSCs (wild-type $n = 11$, *Ash1l*$^{GT/GT}$ $n = 22$; data from individual mice, with mean shown, pooled from 2 experiments, $^{***}P < 0.001$, *t* test). (**E**) Survival after noncompetitive BM transplantation, showing only partial radioprotection by *Ash1l*$^{GT/GT}$ BM ($n = 17$ mice per genotype from 2 experiments; 8 mice for no BM transplantation control). (**F**) Flow cytometric analysis of surviving *Ash1l*$^{GT/GT}$ recipients, showing exclusively host-derived LSK cells. Control *Ash1l*$^{+/+}$ recipients were reconstituted with CD45.2$^+$ donor-derived progenitors (representative of 3 mice per genotype from 2 experiments).

birth. At this stage, *Ash1l*$^{GT/GT}$ mice had a normal frequency of phenotypically defined LT-HSCs in the BM, indicating preserved initial homing from the liver (Figure 6, A and B, and data not shown). However, P19 *Ash1l*$^{GT/GT}$ HSCs showed increased expression of CD34 (Figure 6B). In mice, CD34 is upregulated in cycling HSCs and marks fetal but not the most quiescent adult mouse LT-HSCs (3, 10). To test whether *Ash1l*$^{GT/GT}$ BM HSCs aberrantly maintained a fetal program, we used a *Sox17-GFP* reporter to study expression of *Sox17*, a master regulator of fetal HSCs (11). *Ash1l*$^{GT/GT}$ HSCs were Sox17-GFP$^+$ in the fetal liver and extinguished *Sox17* expression by 2 weeks after birth (Figure 6C). A similar pattern was observed for *Lin28b* transcripts, which were detected in fetal HSCs, as previously reported (12), but absent in both wild-type and *Ash1l*$^{GT/GT}$ adult HSCs (Figure 6C). Thus, *Ash1l* deficiency did not result in the maintenance of a global fetal HSC state.

We next assessed cell cycle status in *Ash1l*$^{GT/GT}$ HSCs. As shown by Ki67/DAPI staining, P19 *Ash1l*$^{GT/GT}$ HSCs had a markedly reduced G_0 fraction, increased entry into G_1, and a trend for more HSCs in $S/G_2/M$ phases of the cell cycle (Figure 6D). Since most HSCs exit the cell cycle in the BM between P14 and P21 (1), this suggested that *Ash1l*-deficient HSCs failed to establish a quiescent stem cell pool at the fetal to adult transition. P19 *Ash1l*$^{GT/GT}$ LT-HSCs but not total BM or c-KIT^{hi}SCA1^{hi} cells also showed increased BrdU incorporation (Supplemental Figure 5). Recent work showed that BM HSC

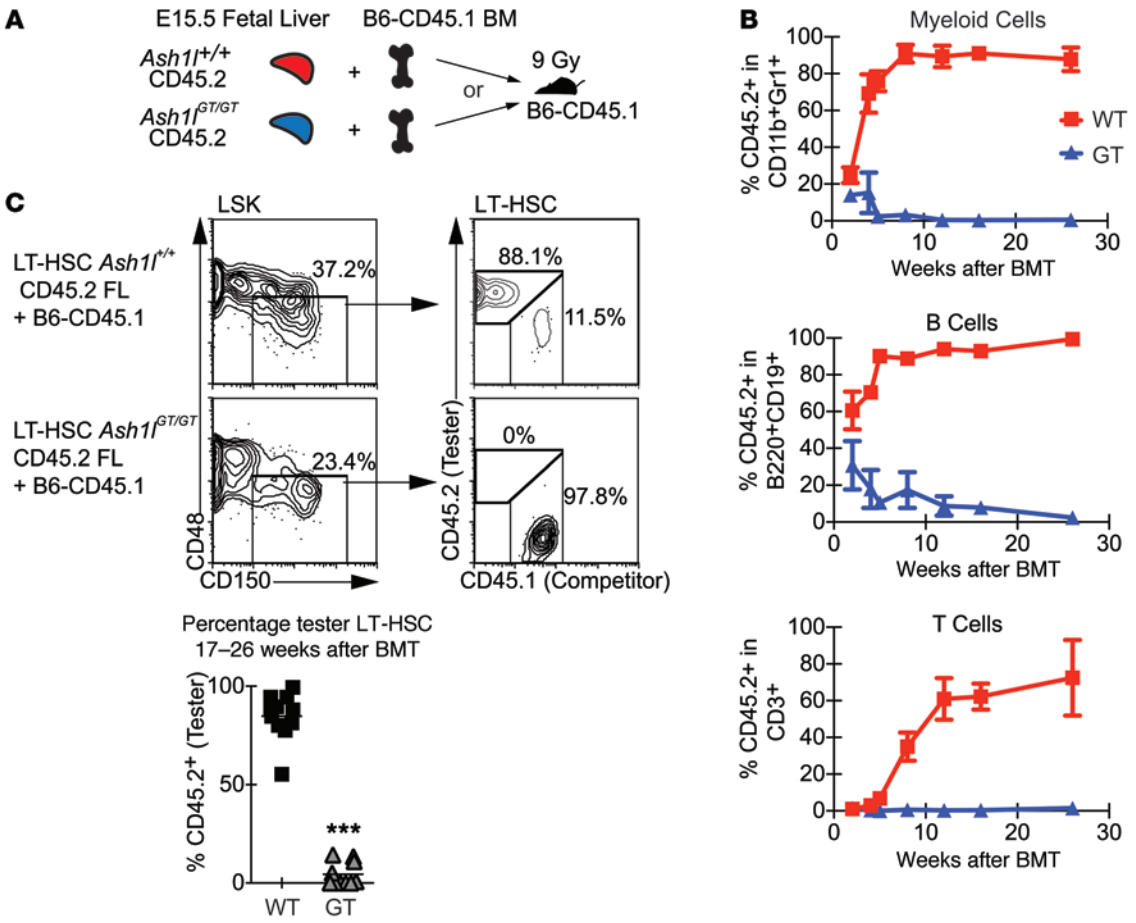

Figure 4. *Ash1l*-deficient fetal liver cells do not sustain long-term BM reconstitution after competitive transplantation. (**A**) Experimental strategy: *Ash1l*$^{+/+}$or *Ash1l*$^{GT/GT}$ B6-CD45.2 E15.5 fetal liver was mixed with wild-type B6-CD45.1 competitor BM (1:1 ratio; 2.5 × 10^5 cells each) and injected into lethally irradiated (9 Gy) B6-CD45.1 recipients. (**B**) Analysis of peripheral blood 2–26 weeks after transplantation, showing a profound reduction of *Ash1l*$^{GT/GT}$ contribution to myeloid, B, and T lineage reconstitution (n = 10–11 mice per genotype; mean ± SD from 2 experiments). (**C**) CD45.2/CD45.1 chimerism in CD150$^+$CD48$^-$LSKs (LT-HSCs) 17–26 weeks after transplantation, showing markedly decreased fetal liver–derived *Ash1l*$^{GT/GT}$ LT-HSCs (wild-type n = 11, *Ash1l*$^{GT/GT}$ n = 10 mice, ***P < 0.001, t test; horizontal bars show the mean).

quiescence is dependent on combined effects of the cyclin-dependent kinase inhibitors p27 (encoded by *Cdkn1b*) and p57 (encoded by *Cdkn1c*) (15, 47). *Ash1l*$^{GT/GT}$ BM LSK cells had markedly decreased expression of these two critical regulators (Figure 6E). Expression of p21 (encoded by *Cdkn1a*) was not altered. These data suggest that *Ash1l* directly or indirectly regulates p27 and p57 expression during establishment of quiescence in young adult HSCs.

We next challenged *Ash1l*$^{GT/GT}$ and control mice with 5-fluorouracil (5-FU) (Figure 7A). 5-FU treatment is toxic to dividing cells but spares quiescent cells, including many normal LT-HSCs. A single 5-FU treatment resulted in a 2-log reduction of *Ash1l*$^{GT/GT}$ LT-HSCs compared with controls, thereby worsening LT-HSC loss in *Ash1l*$^{GT/GT}$ mice by 10- to 20-fold (Figure 7B). This was consistent with increased sensitivity of *Ash1l*$^{GT/GT}$ HSCs to 5-FU, due, at least in part, to decreased quiescence. Consistent with these findings, 5-FU administration was associated with impaired survival of *Ash1l*-deficient mice, even after administration of a single dose (Figure 7, C and D).

Increased cumulative proliferation of hematopoietic progenitors compensates for HSC loss in Ash1l-deficient mice. HSC loss and profound defects in transplantation assays contrasted with preservation of hematopoietic output under steady-state conditions in *Ash1l*-deficient mice. To explore this paradox, we used a pulse-chase H2B-GFP–labeling system to study proliferation history of phenotypically defined HSCs as well as downstream progenitors that normally have limited self-renewal potential (Figure 8A and ref. 8). This strategy allows tetracycline-induced expression of H2B-GFP in all cells (pulse), followed by dilution of GFP fluorescence upon cell division after tetracycline withdrawal (chase). *Ash1l*$^{GT/GT}$ LT-HSCs had increased proliferation throughout the 6-week chase period, as indicated by enhanced GFP dilution (Figure 8B). The entire *Ash1l*$^{GT/GT}$ LSK compartment had markedly increased proliferation as compared with control LSK cells. We could not detect a residual population of LSK or Lin$^-$ cells with high GFP fluorescence in *Ash1l*-deficient mice, consistent with the absence of highly quiescent progenitors (Figure 8B). In contrast, we observed a markedly increased proportion of *Ash1l*$^{GT/GT}$ Lin$^-$GFP$^-$ cells that had preserved a primitive LSK phenotype after 6 weeks of chase (Figure 8C). These findings suggest that increased self-renewal of progenitors downstream of HSCs could compensate for LT-HSC loss and sustain hematopoietic output in *Ash1l*$^{GT/GT}$ mice.

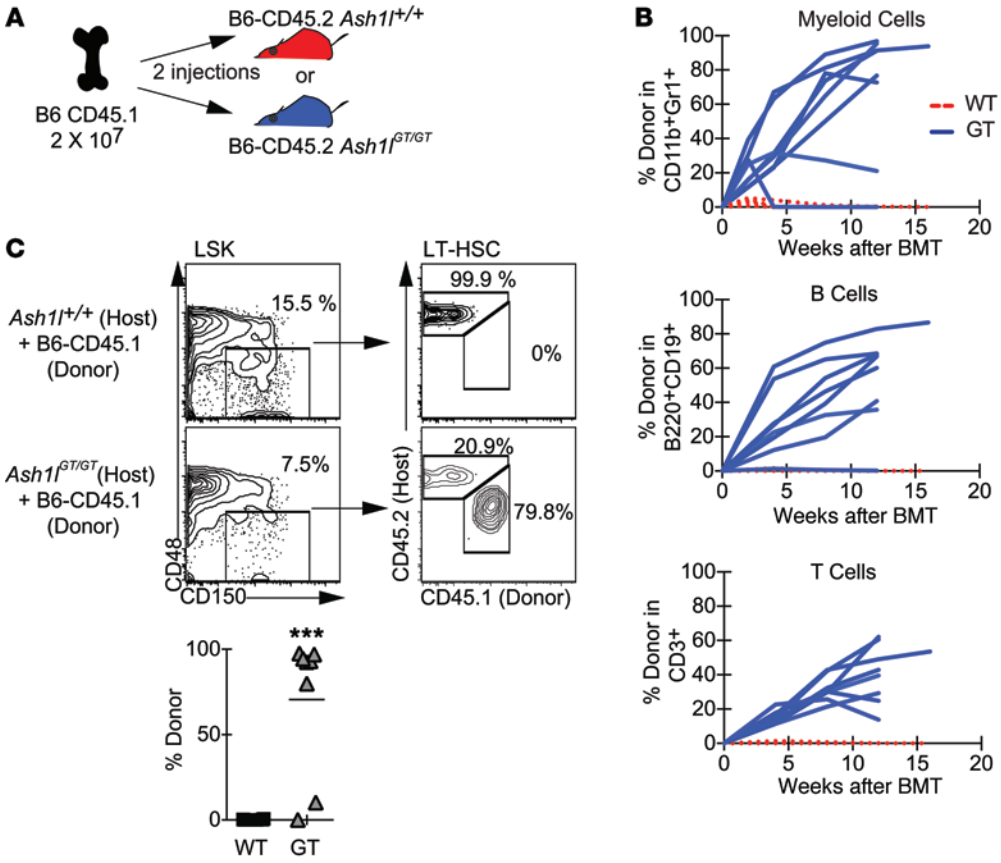

Figure 5. *Ash1l* deficiency allows engraftment of wild-type HSCs in the absence of myeloablation. (**A**) Experimental strategy: B6-CD45.2 *Ash1l*$^{+/+}$ or *Ash1l*$^{GT/GT}$ mice received 2 × 10^7 B6-CD45.1 or B6-GFP BM cells (2 doses 1 week apart i.v.), without prior irradiation. (**B**) Analysis of peripheral blood, showing myeloid, B, and T cell output from CD45.1$^+$ donor BM in 7 of 8 *Ash1l*$^{GT/GT}$ recipients versus 0 of 6 *Ash1l*$^{+/+}$ recipients (data from 3 experiments). Lines represent individual recipients. Reconstitution was sustained for ≥12 weeks. (**C**) Flow cytometric analysis of LT-HSCs 12 to 21 weeks after infusion, showing donor LT-HSC engraftment in 7 of 8 *Ash1l*$^{GT/GT}$ recipients versus 0 of 6 wild-type recipients (pooled from 3 experiments, with horizontal bars showing the mean; ***$P < 0.001$, *t* test).

Ash1l regulates the expression of multiple Hox genes. In flies, TrxG members collaborate to maintain Hox gene expression during development. We reasoned that, if mammalian TrxG members cooperated with one another, they might also share target genes and functional effects. *Mll1*, the mammalian homolog of fly trithorax, regulates expression of multiple Hoxa genes and Hox-related genes, such as *Meis1*. *Ash1l*$^{GT/GT}$ LSK progenitors had reduced expression of *Hoxa3*, *Hoxa4*, *Hoxa5*, *Hoxa6*, *Hoxa9*, *Hoxa10*, and *Meis1* (Figure 9). Thus, *Ash1l* and *Mll1* might share multiple target genes, including Hox genes (25, 48–50). Of note, the expression of *Mll1* itself and that of other genes previously associated with HSC homing and niche retention (*Rac1*, *Rac2*, *Dnmt1*) was not changed (refs. 51, 52, and data not shown).

Ash1l cooperates with Mll1 and Men1 to maintain hematopoiesis. To further explore the functional cooperativity of *Ash1l* and *Mll1* in hematopoiesis, we bred *Ash1l*$^{GT/+}$ mice with *Mll1*$^{fl/fl}$*Mx1-Cre*$^+$ mice, using a conditional *Mll1* allele reported to induce only mild hematopoietic defects upon inactivation in steady-state conditions (26). This strategy allowed deletion of one or both *Mll1* alleles via poly(I:C) injection in the presence of graded *Ash1l* doses (Figure 10A). Combined *Mll1* and *Ash1l* deficiency resulted in rapid and profound reduction in BM cellularity, suggesting hematopoietic failure (Figure 10B). Flow cytometric analysis of LT-HSCs and hematopoietic progenitors showed that *Ash1l*$^{GT/GT}$ *Mll1*$^{fl/fl}$*Mx1-Cre*$^+$ mice had profound reductions in both LT-HSCs and LSK progenitors (Figure 10, C and D). In addition, we observed a unique sensitivity of LT-HSCs to the combined *Mll1* and *Ash1l* gene dose, as numbers of LT-HSCs decreased more profoundly when homozygous *Ash1l* or *Mll1* inactivation was combined with heterozygous inactivation of *Mll1* or *Ash1l*, respectively (Figure 10C). CD34$^-$ LT-HSCs, a highly quiescent adult HSC subset identified with surface markers in mice, were particularly sensitive to inactivation of an increasing number of *Ash1l* and *Mll1* alleles (Figure 10D), suggesting that *Ash1l* and *Mll1* cooperate to maintain quiescent HSCs. However, multipotent progenitors and overall BM cellularity were only depleted upon targeting of both *Mll1* and *Ash1l* alleles (Figure 10, B–D). Finally, we assessed the combined effects of *Ash1l* deficiency and inactivation of *Men1*, encoding the MLL1 cofactor menin (Supplemental Figure 6). Menin is essential for recruitment of the MLL1 complex, at least to a subset of target genes, and was previously shown to regulate HSC homeostasis (53–55). Profound thrombocytopenia, BM hypocellularity, and loss of all hematopoietic progenitors were observed upon combined deficiency of both *Ash1l* and *Men1* alleles but not when even one of the four alleles was maintained (Supplemental Figure 6, B–D). LT-HSCs were particularly sensitive to graded loss of *Ash1l* and *Men1* alleles. (Supplemental Figure 6D). Although only some *Mll1* target genes are sensitive to *Men1* loss (50), these genes may be important for the cooperative effects of *Ash1l* and *Mll1* in hematopoiesis. Together, these findings reveal cooperativity between *Ash1l* and *Mll1* or *Men1* in HSCs and hematopoietic progenitor cells, uncovering a unique sensitivity of quiescent adult HSCs to regulation by the TrxG family.

Discussion

Our findings uncover an essential function for the TrxG gene *Ash1l* in the regulation of adult HSCs and reveal functional cooperativity of TrxG members in hematopoiesis. When *Ash1l* levels were

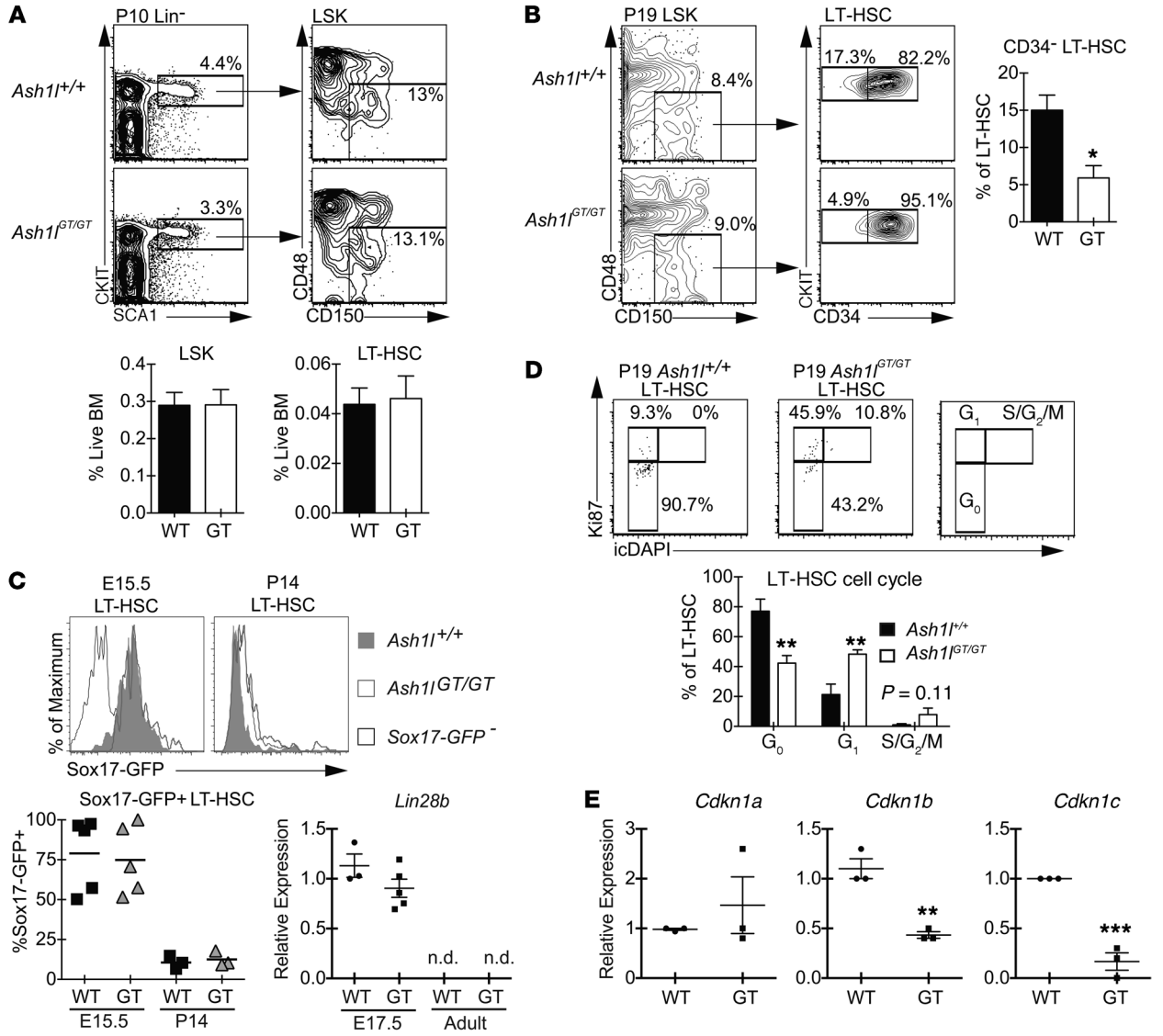

Figure 6. *Ash1l*$^{GT/GT}$ LT-HSCs home to the BM but fail to establish normal quiescence, despite appropriate extinction of the fetal HSC program. (**A**) Flow cytometric analysis of P10 BM, showing comparable frequencies of phenotypically defined LT-HSCs (CD150$^+$CD48$^-$LSK) in *Ash1l*$^{GT/GT}$ and *Ash1l*$^{+/+}$ littermates (≥9 mice per genotype; mean ± SEM). (**B**) Decreased percentage of quiescent CD34$^-$ cells in *Ash1l*$^{GT/GT}$ LT-HSCs (P19) (4 mice per genotype; mean ± SEM). (**C**) Sox17-GFP expression in E15.5 fetal liver and P14 BM LT-HSCs (CD150$^+$CD48$^-$LSK cells). Sox17-GFP was present in fetal LT-HSCs but extinguished in wild-type and *Ash1l*$^{GT/GT}$ P14 BM ($n \geq 3$ per genotype, 4 experiments; symbols show individual mice and the bars show the mean). qRT-PCR analysis shows similar *Lin28b* gene expression in *Ash1l*$^{GT/GT}$ and *Ash1l*$^{+/+}$ fetal LSK progenitors, with loss of expression in adult progenitors of both genotypes (n = 3–5 per group; mean ± SEM) (n.d., not detectable). (**D**) Flow cytometry plots (Ki67 vs. DAPI) showing decreased G_0 (quiescent fraction) and increased distribution into G_1 and $S/G_2/M$ phases of the cell cycle in P19 *Ash1l*$^{GT/GT}$ LT-HSCs (5 mice per genotype; mean ± SEM). (**E**) Reduced *Cdkn1b* and *Cdkn1c* expression relative to *Hprt1* in P10 *Ash1l*$^{GT/GT}$ LSK progenitors (qRT-PCR, n = 3 per group, mean ± SEM). $^*P < 0.05$, $^{**}P < 0.01$, $^{***}P < 0.001$, t test.

profoundly reduced in *Ash1l*$^{GT/GT}$ mice, the ability of young adult LT-HSCs to establish and maintain quiescence was impaired. *Ash1l*-deficient HSCs developed and expanded normally in the fetal liver and initially seeded the BM. Once in the BM, these LT-HSCs did not upregulate expression of *Cdkn1b/c*, which was associated with reduced numbers of quiescent HSCs. Because fetal HSCs are known to divide rapidly, these results could have arisen from the persistence of a fetal program upon reaching the BM. However, expression of *Sox17* and *Lin28b*, two essential regulators of the fetal HSC transcriptional program, was properly extinguished in BM *Ash1l*$^{GT/GT}$ LT-HSCs, indicating that their reduced ability to establish quiescence occurred despite transition from fetal to adult state. Altogether, we believe that *Ash1l* is a novel key regulator of changes associated with the adaptation of HSCs to the BM niche at the fetal to adult transition or upon transplantation of HSCs into an adult recipient.

Ash1l$^{GT/GT}$ BM had profoundly reduced LT-HSC numbers but maintained relatively normal mature hematopoietic cell output. This paradox did not result from the presence of phenotypically abnormal but functional HSCs residing in the *Ash1l*$^{GT/GT}$ BM, as young adult *Ash1l*$^{GT/GT}$ BM failed to achieve long-term reconstitution in irradiated recipients after competitive and noncom-

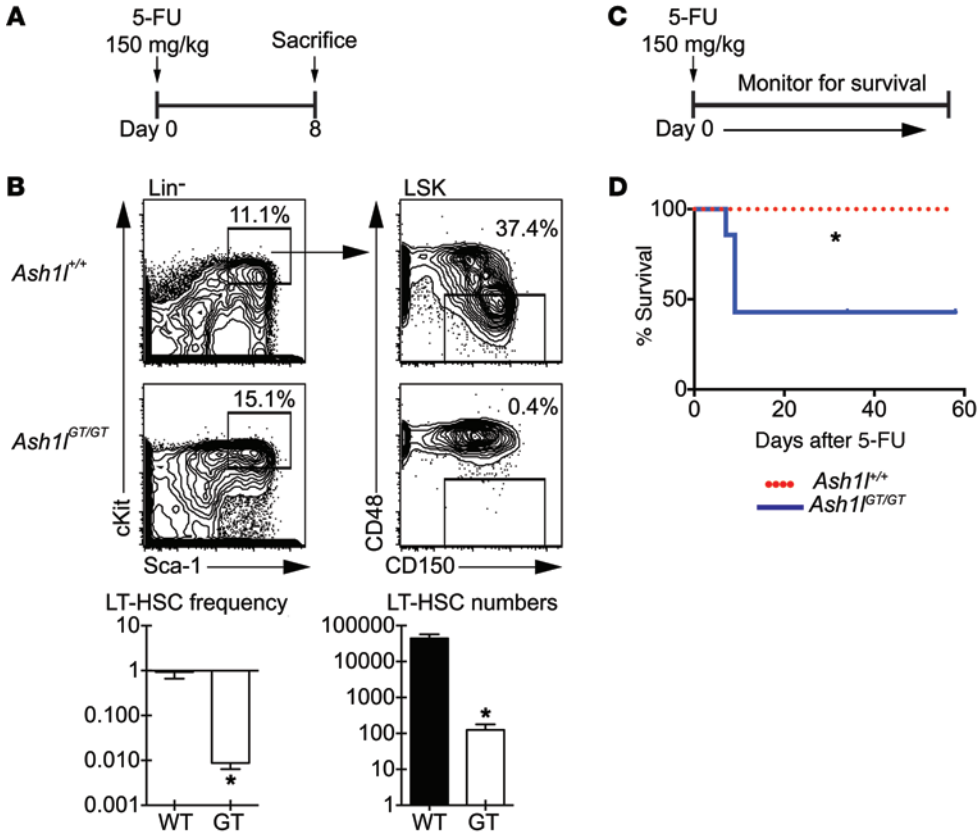

Figure 7. *Ash1l*$^{GT/GT}$ mice are more sensitive to 5-FU challenge than wild-type mice. (**A**) Experimental strategy: mice of indicated genotypes were injected with 150 mg/kg 5-FU and sacrificed 8 days later. (**B**) Flow cytometric analysis of LT-HSCs ($CD150^+CD48^-$LSK cells), showing 2-log reduction in frequency and 2.5-log reduction in LT-HSC numbers in *Ash1l*$^{GT/GT}$ mice as compared with control mice after 5-FU exposure ($n \geq 4$ mice per genotype; mean ± SEM, $^*P < 0.05$, *t* test). (**C**) Experimental strategy: mice were injected with 150 mg/kg 5-FU and monitored for survival. (**D**) Survival of mice after 5-FU challenge (7 mice per genotype, representative of 2 experiments, $^*P < 0.05$, log-rank Mantel-Cox test).

petitive transplantation. Based on this gold standard approach of HSC biology, we could not detect LT-HSC function in the *Ash1l*$^{GT/GT}$ BM, indicating that the presence of functional HSCs with an alternative phenotype was unlikely. Furthermore, we could also not detect functional LT-HSCs after transplantation of *Ash1l*$^{GT/GT}$ fetal liver progenitors, which had LT-HSC frequency comparable to that of *Ash1l*$^{+/+}$ mice by phenotypic criteria. Thus, despite their normal in vivo expansion in the fetal/neonatal liver, *Ash1l*$^{GT/GT}$ LT-HSCs could not establish durable hematopoiesis in the BM niche after transplantation, indicating that they were functionally abnormal, even if they expanded normally in the fetal environment. As normal numbers of *Ash1l*$^{GT/GT}$ HSCs were initially present in the neonatal BM, our data are consistent with preserved HSC homing to the BM in these mice but also with failure to respond to niche factors that are required for the establishment of quiescence and subsequent stable engraftment. Among putative essential niche-derived factors in the BM, thrombopoietin (TPO) and TGF-β have been linked to induction of quiescence through *Cdkn1b/c* upregulation (14, 56, 57). Furthermore, decreased expression of multiple posterior Hoxa genes was observed in young adult HSCs of TPO-deficient mice (14). Thus, *Ash1l* may be necessary to establish a normal transcriptional response downstream of TPO or other essential BM niche factors required for adult HSC quiescence, maintenance, and function. As genetic inactivation of *Hoxa9* and other Hoxa genes was shown to cause HSC defects, we speculate that decreased expression of multiple Hoxa genes accounts for part of the defects in *Ash1l*-deficient HSCs, although other factors are likely involved as well (58, 59).

Ash1l-deficient mice did not progress to frank hematopoietic failure, despite severe depletion of phenotypically defined LT-HSCs and lack of transplantable HSCs. A possible explanation for these findings is that few residual LT-HSCs could maintain steady-state hematopoiesis through a compensatory increase in proliferation. Using H2B-GFP in a pulse-chase system (8), we indeed observed increased cumulative proliferation of all primitive *Ash1l*$^{GT/GT}$ hematopoietic progenitors, consistent with the absence of a slowly cycling progenitor pool. A striking feature of *Ash1l*-deficient hematopoiesis, however, was the large increase in cells that maintained a primitive LSK phenotype, despite the complete loss of GFP at the end of the chase period. Thus, *Ash1l*-deficient progenitors downstream of LT-HSCs showed evidence of increased self-renewal in vivo in the absence of a normal HSC compartment. This phenomenon is reminiscent of recent observations that early thymocyte progenitors acquire extended self-renewal in vivo when the normal input of blood-derived T lineage progenitors is impaired, suggesting that self-renewal potential can be modulated in individual hematopoietic progenitors as an adaptation to pathological conditions (60, 61). It is interesting to speculate about why compensatory changes in *Ash1l*-deficient mice were not sustained after transplantation into irradiated recipients. Emerging evidence indicates that steady-state hematopoiesis and stress hematopoiesis after transplantation are regulated by different mechanisms (62). After transplantation, hematopoiesis is driven by a small number of LT-HSCs that outcompete other progenitors, while steady-state hematopoiesis can be maintained for extended periods of time by a broader range of downstream progenitors with more

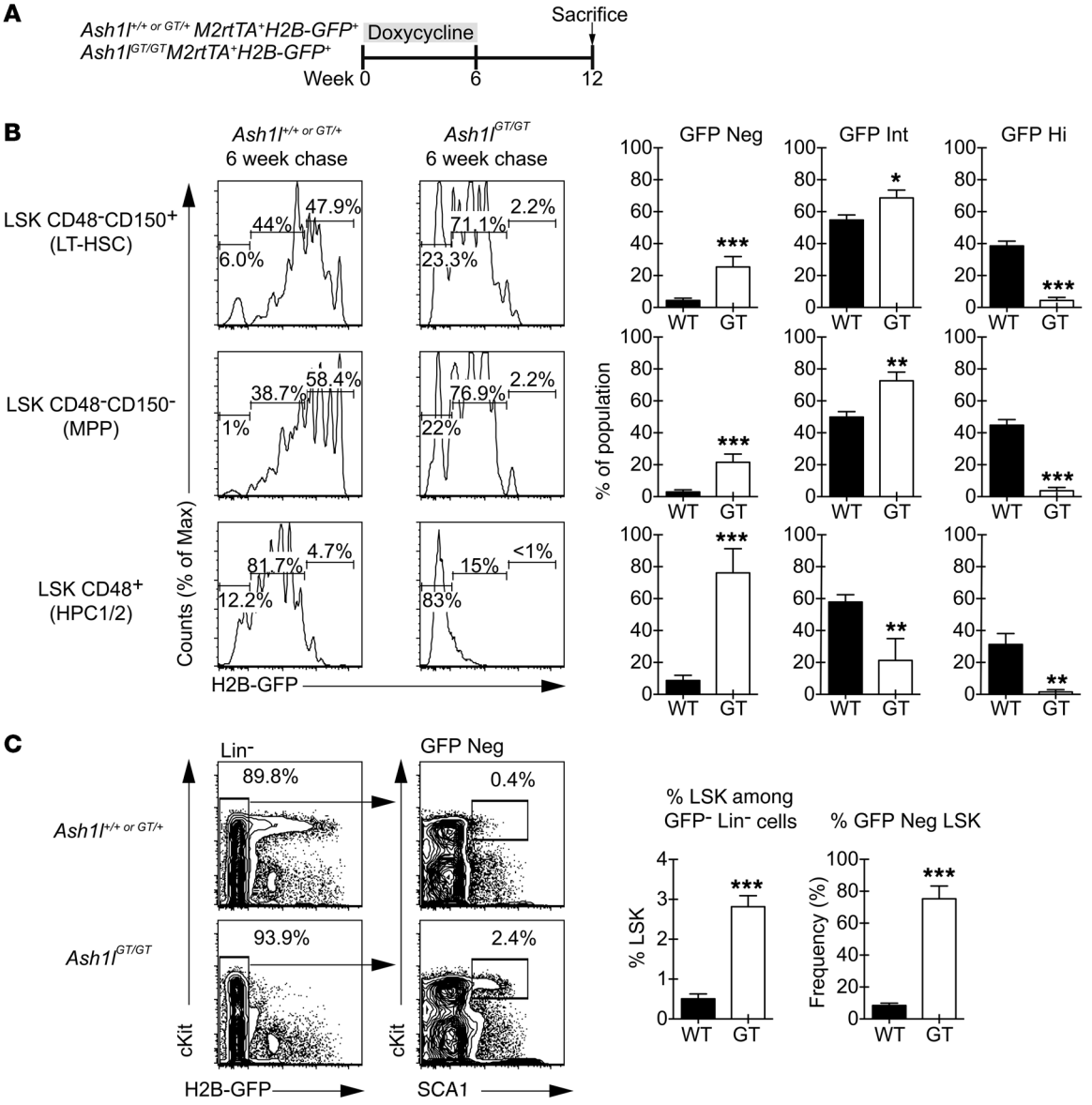

Figure 8. In vivo proliferation history shows decreased quiescence of *Ash1l*-deficient HSCs but increased persistence of proliferating downstream progenitors. (**A**) Experimental strategy: *Ash1l*$^{+/+}$ or *Ash1l*$^{GT/GT}$ mice with *M2rtTA* and *H2B-GFP* transgenes were maintained on doxycycline for 6 weeks to label hematopoietic cells with GFP. GFP dilution was monitored by flow cytometry after a 6-week chase period. (**B**) Flow cytometric analysis after chase, showing significantly increased GFP dilution in *Ash1l*$^{GT/GT}$ LSK CD150$^+$CD48$^-$ cells (containing LT-HSCs), LSK CD150$^-$CD48$^-$ (MPP), and LSK CD48$^+$ progenitors (HPC1/2) compared with controls, consistent with increased cell division (≥6 mice per genotype; mean ± SEM). (**C**) Flow cytometric analysis, demonstrating that the H2B-GFP–negative fraction of Lin$^-$ cells was enriched for primitive LSK progenitors in *Ash1l*$^{GT/GT}$ versus *Ash1l*$^{+/+}$ mice (≥ 4 mice per genotype; mean ± SEM). **P* < 0.05, ***P* < 0.01, ****P* < 0.001, *t* test.

restricted potential. Thus, it is possible that *Ash1l*-deficient mice were competent for this type of hematopoiesis but selectively deficient in LT-HSC function after transplant.

Only a few genetic models of HSC dysfunction that support nonablative transplantation have been reported in hematopoietic biology (52, 63). In *Ash1l*$^{GT/GT}$ mice, successful engraftment in nonablative transplantation experiments suggested that the *Ash1l*-deficient BM niche was not defective, as it could support maintenance of wild-type LT-HSCs. Stable wild-type LT-HSC engraftment suggested that niche spaces were available due to LT-HSC depletion and/or that remaining *Ash1l*$^{GT/GT}$ LT-HSCs competed poorly for niche space. Either scenario is consistent with extreme LT-HSC dysfunction when *Ash1l* levels are reduced. Of note, the full effects of *Ash1l* could be even more profound than observed in *Ash1l*$^{GT/GT}$ mice, as these mice had low residual levels of normal *Ash1l* transcripts, consistent with *Ash1l*^{GT} being a severely hypomorphic but not a null allele.

Cooperative effects of *Mll1* and *Ash1l* in hematopoiesis highlight an evolutionarily conserved feature of TrxG members, a phenomenon identified in flies but not previously described in mammals. Loss of a single *Ash1l*^{GT} allele amplified LT-HSC depletion in *Men1*-deficient and *Mll1*-deficient mice, while complete

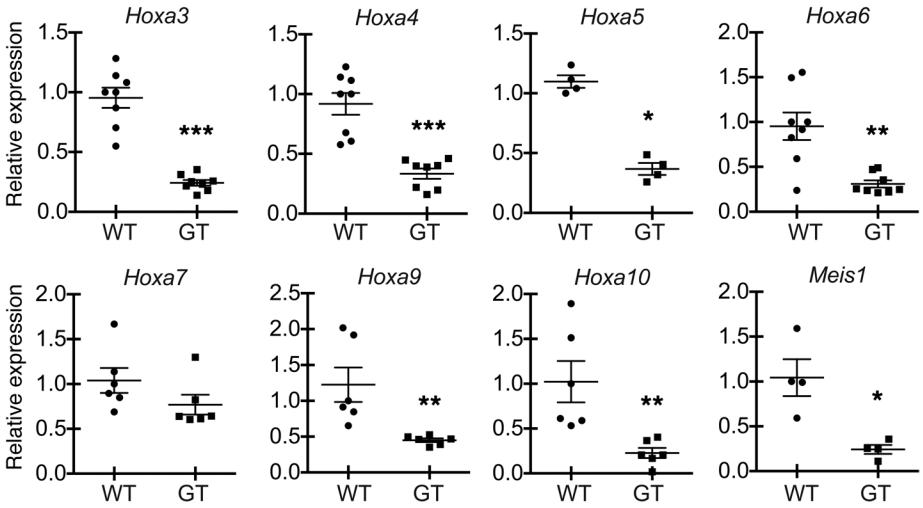

Figure 9. *Ash1l* regulates expression of *Hox* and *Hox*-related genes in hematopoietic progenitors. Relative abundance of Hoxa and *Meis1* normalized to *Hprt1* transcripts in sort-purified adult $Ash1l^{GT/GT}$ LSK progenitors, as assessed by qRT-PCR (triplicate analysis of 4 to 8 individual biological samples per genotype, mean ± SEM; $^{*}P < 0.05$, $^{**}P < 0.01$, $^{***}P < 0.001$, *t* test).

hematopoietic failure was observed only when all 4 alleles were deficient. This dominant phenotypic enhancement is reminiscent of criteria used to identify TrxG members in *Drosophila*. To date, the biochemical mechanisms underlying this genetic observation remain poorly understood. Given that both *Mll1* and *Ash1l* are required for Hox gene expression, it is possible that MLL1 and ASH1L proteins act nonredundantly to promote transcription at a shared subset of target genes. Indeed, both $Ash1l^{GT/GT}$ and *Mll1*- or *Men1*-deficient hematopoietic progenitors displayed a reduced, but not absent, expression of posterior Hoxa genes, suggesting multifactorial regulation at this locus (25, 50, 54). Since MLL1 and ASH1L SET domains have H3K4 and H3K36 methyltransferase activity, two histone marks that are involved in transcription initiation and elongation steps, respectively, it can be envisioned that they target different regulatory steps of transcription. In this scenario, either *Mll1* or *Ash1l* inactivation can lead to compromised Hoxa gene expression. It also remains to be determined whether the cooperative interaction between *Mll1* and *Ash1l* is limited to the regulation of Hoxa genes in LT-HSCs, especially since *Mll1* was reported to control multiple other genes in normal hematopoiesis (50). Future work should explore the detailed molecular mechanisms by which TrxG members cooperatively regulate quiescent adult HSCs.

Methods

Mice. C57BL/6.Ptprca (B6-SJL, $CD45.1^{+}$) mice were from the National Cancer Institute. B6-GFP transgenic mice expressing GFP under the control of the human ubiquitin C promoter were from The Jackson Laboratory (64). $Ash1l^{GT/+}$ embryonic stem cells were obtained from Sanger Institute. After blastocyst injection, $Ash1l^{GT/+}$ mice were generated by the University of Michigan Transgenic Animal Core and intercrossed. In most experiments, $Ash1l^{GT/+}$ mice were backcrossed to the C57BL/6 background (B6, $CD45.2^{+}$) for at least 6 generations. In selected experiments, $Ash1l^{GT/+}$ mice were bred with $Sox17^{GFP/+}$ mice, with transgenic mice containing both *Rosa26-rtTA* and *TetOP-H2B-GFP*, with $Men1^{fl/fl}Mx1\text{-}Cre^{+}$ mice or with $Mll1^{fl/fl}$ $Mx1\text{-}Cre^{+}$ mice (8, 11, 26, 65, 66). To label hematopoietic cells with H2B-GFP, *Rosa26-rtTA TetOP-H2B-GFP* mice were maintained on doxycycline (2 mg/ml in drinking water) for 6 weeks. Mice were maintained on normal water for a chase period (6 weeks) to allow GFP dilution in dividing cells. *Men1* or *Mll1* excision was achieved with poly(I:C) (Amersham; 50 μg i.p. every 2 days for 5 doses).

Flow cytometry. Single cell suspensions were prepared from fetal liver, BM, or blood, followed by red blood cell lysis (ACK buffer, Cambrex). The following antibodies were from BioLegend: anti-CD3, anti-CD4, anti-CD8, anti-CD11b, anti-CD11c, anti-CD19, anti-CD48, anti-CD150, anti-Gr1/Ly-6G, anti-B220, anti-NK1.1, anti-TCRβ, anti-TCRγδ, and anti-cKIT. Anti-SCA1 was from eBiosciences. We used the following antibody cocktail to exclude $lineage^{+}$ cells: anti-CD11b, anti-Gr1, anti-CD11c, anti-B220, anti-CD19, anti-CD3, anti-TCRβ, anti-TCRγδ, anti-CD8, anti-NK1.1, and anti-Ter119. In fetal samples, CD11b was omitted. BrdU analysis was performed using a BrdU Labeling Kit (BD Biosciences). Ki67 staining was achieved using the BD Ki67 Set (BD Biosciences). Analysis was performed on a FACSCanto and sorting was performed on a FACSAria II/III (BD Biosciences). Dead cells were excluded with 4′6-diamidino-2-phenylindole (Sigma-Aldrich). Flow cytometry files were analyzed with FlowJo (TreeStar).

BM and fetal liver cell transplantation. Six- to eight-week-old B6-SJL ($CD45.1^{+}$) mice were lethally irradiated (900 Gy, ^{37}Cs source). Four hours after irradiation, mice were transplanted with 6- to 10-week-old donor BM or E15.5 fetal liver cells via tail vein injection. For competitive transplantation, we mixed equal numbers of competitor B6-SJL BM and tester $CD45.2^{+}$ BM or fetal liver cells. For nonablative transplantation, 5- to 8-week-old $Ash1l^{GT/GT}$ mice or wild-type controls were injected twice at 1-week intervals with 2.0×10^{7} B6-SJL ($CD45.1^{+}$) or B6-GFP ($CD45.2^{+}$) BM cells. For BM homing studies, recipients were analyzed 24 hours after transplantation.

Complete blood counts. Blood was obtained through retroorbital bleeding and transferred to EDTA-treated tubes. Complete blood counts were determined using the Advia 120 Hematology System (Siemens).

CFU-GM. 20,000 BM cells or 200,000 spleen cells were plated per ml of MethoCult GF M3534 (Stem Cell Technologies). Colonies were scored 7 to 10 days later.

Quantitative real-time PCR. For gene expression analyses, at least 5,000 cells from each population of interest were sort purified directly into Trizol (Invitrogen). After RNA extraction, cDNA was generated using the SuperScript III First-Strand Synthesis Kit (Invitrogen) or the Nugen

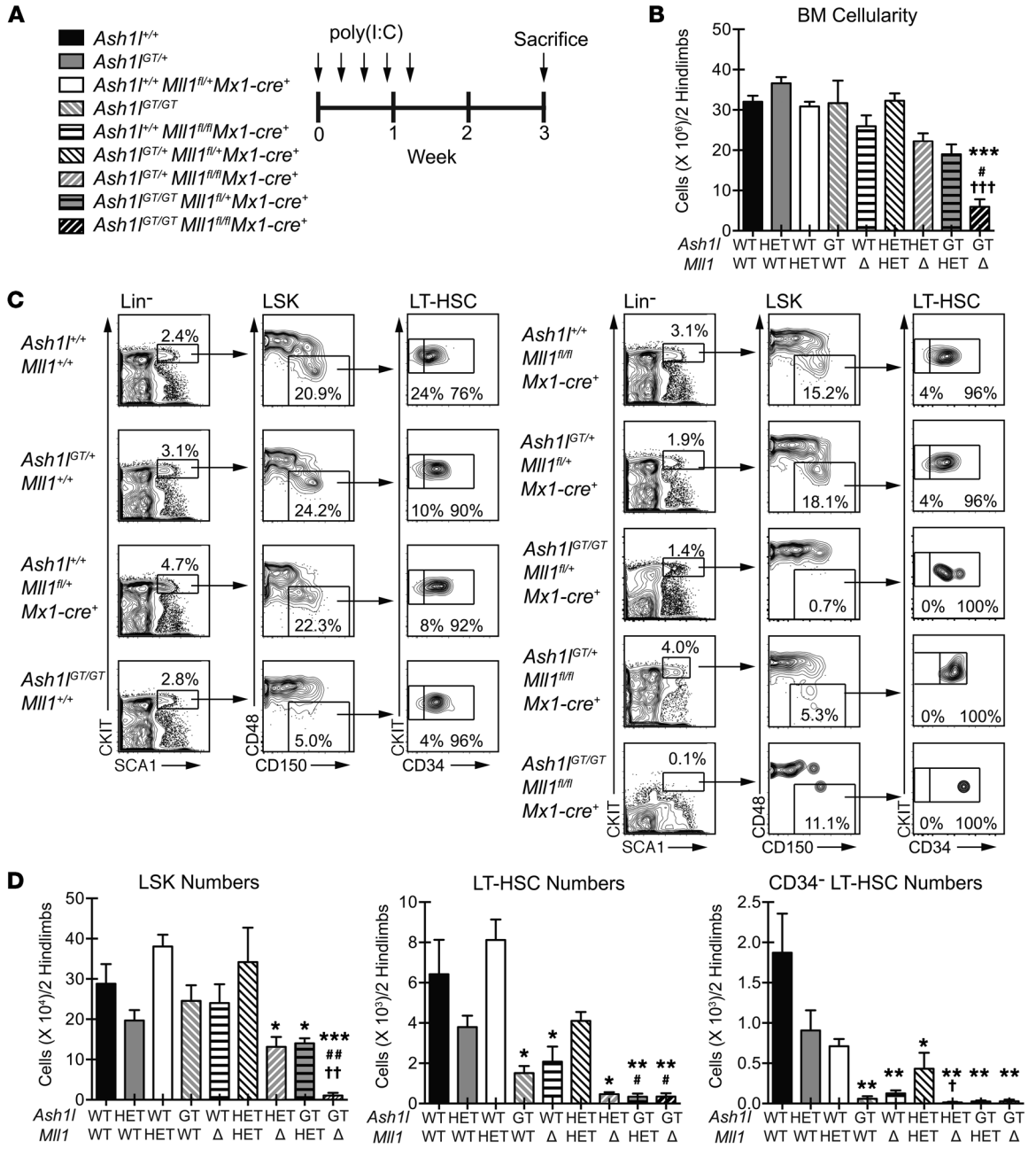

Figure 10. Combined *Ash1l* and *Mll1* deficiency induces overt hematopoietic failure and profound depletion of LT-HSCs and LSK progenitors. (**A**) Experimental strategy: mice of indicated genotypes were injected with poly(I:C) (20 μg every 2 days 5 times). (**B**) Reduced BM cellularity in *Ash1l*$^{GT/GT}$ *Mll1*$^{fl/fl}$*Mx1-Cre*$^{+}$mice (≥2 mice per genotype; mean ± SEM). (**C**) Flow cytometric analysis showing severe reduction in CD34^{-} LT-HSCs, LT-HSCs, and LSK progenitors in *Ash1l*$^{GT/GT}$ *Mll1*$^{fl/fl}$*Mx1-Cre*$^{+}$mice and reduced CD34^{-}LT-HSC and LT-HSC frequency with cumulative inactivation of *Ash1l* and *Mll1* alleles. The representative plot for *Ash1l*$^{GT/+}$ *Mll1*$^{fl/fl}$*Mx1-Cre*$^{+}$ BM is derived from a separate experiment, thus gating definitions differ from the other samples. (**D**) LSK and LT-HSC numbers, reflecting hematopoietic failure in *Ash1l*$^{GT/GT}$ *Mll1*$^{fl/fl}$*Mx1-Cre*$^{+}$ mice and LT-HSC sensitivity to loss of *Ash1l* and *Mll1* alleles (≥2 mice per genotype; mean ± SEM), and CD34^{-} LT-HSC numbers in 2 hind legs, showing high sensitivity of this population to regulation by TrxG members. $^{*}P < 0.05$, $^{**}P < 0.01$, $^{***}P < 0.001$, compared with wild type; $^{\#}P < 0.05$, $^{\#\#}P < 0.01$, compared with *Ash1l*$^{GT/GT}$; $^{\dagger}P < 0.05$, $^{\dagger\dagger}P < 0.01$, $^{\dagger\dagger\dagger}P < 0.001$, compared with induced *Mll*$^{fl/fl}$ *Mx1-Cre*$^{+}$, *t* test.

Ovation PicoSL WTA System (Nugen Technologies). Relative gene expression was measured using TaqMan primers and probe sets from Applied Biosystems (*Hoxa5*: Mm00439362_m1; *Hoxa7*: Mm00657963_m1; *Hoxa9*: Mm00439364_m1; *Hoxa10*: Mm00433966_m1; *Meis1*: Mm00487664_m1; *Cdkn1a*: Mm00432448_m1; *Cdkn1b*: Mm00438168_m1; *Cdkn1c*: Mm00438170_m1) or SYBR Green (Fisher) with the following primer pairs: *Hoxa3*, AAGCGACCTACTACGACAG and TGGCATTGTAAGCGAACC; *Hoxa4*, CAGAACCGGAGAATGAAGTG and CGAGGCAGTGTTGGAAGA; and *Hoxa6*, TTACCAACAGTCCAACTC and GGTCTTTATCAGAATAGAAACA. Reactions were carried out on a Mastercycler realplex (Eppendorf). Relative expression was calculated after normalization with *Hprt1* expression using the ΔΔCT method.

Statistics. Comparison of two means was performed with 2-tailed unpaired Student's *t* test. Where indicated, we used a log-rank Mantel-Cox test.

Study approval. The University of Michigan Committee on Use and Care of Animals approved all experiments.

Acknowledgments

We are grateful to Hugh J.M. Brady for *Mll1*$^{fl/fl}$ mice, Sean Morrison for *Sox17-GFP* mice, David Ginsburg for *B6-GFP* mice, and Hanno Hock for *Rosa26-rtTA* and *TetOP-H2B-GFP* mice. This work was supported by the Sidney Kimmel Cancer Research Foundation, the University of Michigan Comprehensive Cancer Center, the D. Dan and Betty Kahn Foundation, and the NIH (RO1-AI091627 to I. Maillard, R37-HD30428 to S.A. Camper). Individual support included T32 training grants from the University of Michigan's Medical Scientist Training Program (GM07863 to M. Jones), Center for Organogenesis (HD007505 to M. Jones and J. Chase), and Cellular and Molecular Biology Program (GM007315 to J. Chase). Flow cytometry was partially supported by a core grant from the NIH to the University of Michigan Cancer Center (P30-CA46592).

Address correspondence to: Ivan Maillard, Life Sciences Institute #6382A, 210 Washtenaw Avenue, University of Michigan, Ann Arbor, Michigan 48109, USA. Phone: 734.763.3599; E-mail: imaillar@umich.edu.

1. Bowie MB, McKnight KD, Kent DG, McCaffrey L, Hoodless PA, Eaves CJ. Hematopoietic stem cells proliferate until after birth and show a reversible phase-specific engraftment defect. *J Clin Invest*. 2006;116(10):2808–2816.
2. Ema H, Nakauchi H. Expansion of hematopoietic stem cells in the developing liver of a mouse embryo. *Blood*. 2000;95(7):2284–2288.
3. Wilson A, et al. Hematopoietic stem cells reversibly switch from dormancy to self-renewal during homeostasis and repair. *Cell*. 2008;135(6):1118–1129.
4. Takizawa H, Regoes RR, Boddupalli CS, Bonhoeffer S, Manz MG. Dynamic variation in cycling of hematopoietic stem cells in steady state and inflammation. *J Exp Med*. 2011;208(2):273–284.
5. Venezia TA, et al. Molecular signatures of proliferation and quiescence in hematopoietic stem cells. *PLoS Biol*. 2004;2(10):e301.
6. Cheshier SH, Morrison SJ, Liao X, Weissman IL. In vivo proliferation and cell cycle kinetics of long-term self-renewing hematopoietic stem cells. *Proc Natl Acad Sci U S A*. 1999;96(6):3120–3125.
7. Baldridge MT, King KY, Boles NC, Weksberg DC, Goodell MA. Quiescent haematopoietic stem cells are activated by IFN-γ in response to chronic infection. *Nature*. 2010;465(7299):793–797.
8. Foudi A, et al. Analysis of histone 2B-GFP retention reveals slowly cycling hematopoietic stem cells. *Nat Biotechnol*. 2009;27(1):84–90.
9. Bowie MB, et al. Identification of a new intrinsically timed developmental checkpoint that reprograms key hematopoietic stem cell properties. *Proc Natl Acad Sci U S A*. 2007;104(14):5878–5882.
10. Ito T, Tajima F, Ogawa M. Developmental changes of CD34 expression by murine hematopoietic stem cells. *Exp Hematol*. 2000;28(11):1269–1273.
11. Kim I, Saunders TL, Morrison SJ. Sox17 dependence distinguishes the transcriptional regulation of fetal from adult hematopoietic stem cells. *Cell*. 2007;130(3):470–483.
12. Yuan J, Nguyen CK, Liu X, Kanellopoulou C, Muljo SA. Lin28b reprograms adult bone marrow hematopoietic progenitors to mediate fetal-like lymphopoiesis. *Science*. 2012;335(6073):1195–1200.
13. Fleming WH, Alpern EJ, Uchida N, Ikuta K, Spangrude GJ, Weissman IL. Functional heterogeneity is associated with the cell cycle status of murine hematopoietic stem cells. *J Cell Biol*. 1993;122(4):897–902.
14. Qian H, et al. Critical role of thrombopoietin in maintaining adult quiescent hematopoietic stem cells. *Cell Stem Cell*. 2007;1(6):671–684.
15. Zou P, et al. p57(Kip2) and p27(Kip1) cooperate to maintain hematopoietic stem cell quiescence through interactions with Hsc70. *Cell Stem Cell*. 2011;9(3):247–261.
16. Orford KW, Scadden DT. Deconstructing stem cell self-renewal: genetic insights into cell-cycle regulation. *Nat Rev Genet*. 2008;9(2):115–128.
17. Ringrose L, Paro R. Epigenetic regulation of cellular memory by the Polycomb and Trithorax group proteins. *Annu Rev Genet*. 2004;38:413–443.
18. Shearn A. The ash-1, ash-2 and trithorax genes of Drosophila melanogaster are functionally related. *Genetics*. 1989;121(3):517–525.
19. Tripoulas NA, Hersperger E, La Jeunesse D, Shearn A. Molecular genetic analysis of the Drosophila melanogaster gene absent, small or homeotic discs1 (ash1). *Genetics*. 1994;137(4):1027–1038.
20. Armstrong SA, et al. MLL translocations specify a distinct gene expression profile that distinguishes a unique leukemia. *Nat Genet*. 2002;30(1):41–47.
21. Gu Y, et al. The t(4;11) chromosome translocation of human acute leukemias fuses the ALL-1 gene, related to Drosophila trithorax, to the AF-4 gene. *Cell*. 1992;71(4):701–708.
22. Tkachuk DC, Kohler S, Cleary ML. Involvement of a homolog of Drosophila trithorax by 11q23 chromosomal translocations in acute leukemias. *Cell*. 1992;71(4):691–700.
23. Ziemin-van der Poel S, et al. Identification of a gene, MLL, that spans the breakpoint in 11q23 translocations associated with human leukemias. *Proc Natl Acad Sci U S A*. 1991;88(23):10735–10739.
24. Yu BD, Hess JL, Horning SE, Brown GA, Korsmeyer SJ. Altered Hox expression and segmental identity in Mll-mutant mice. *Nature*. 1995;378(6556):505–508.
25. Jude CD, Climer L, Xu D, Artinger E, Fisher JK, Ernst P. Unique and independent roles for MLL in adult hematopoietic stem cells and progenitors. *Cell Stem Cell*. 2007;1(3):324–337.
26. McMahon KA, et al. Mll has a critical role in fetal and adult hematopoietic stem cell self-renewal. *Cell Stem Cell*. 2007;1(3):338–345.
27. Milne TA, et al. MLL targets SET domain methyltransferase activity to Hox gene promoters. *Mol Cell*. 2002;10(5):1107–1117.
28. Dou Y, et al. Regulation of MLL1 H3K4 methyltransferase activity by its core components. *Nat Struct Mol Biol*. 2006;13(8):713–719.
29. Southall SM, Wong PS, Odho Z, Roe SM, Wilson JR. Structural basis for the requirement of additional factors for MLL1 SET domain activity and recognition of epigenetic marks. *Mol Cell*. 2009;33(2):181–191.
30. Steward MM, Lee JS, O'Donovan A, Wyatt M, Bernstein BE, Shilatifard A. Molecular regulation of H3K4 trimethylation by ASH2L, a shared subunit of MLL complexes. *Nat Struct Mol Biol*. 2006;13(9):852–854.
31. Ruthenburg AJ, et al. Histone H3 recognition and presentation by the WDR5 module of the MLL1 complex. *Nat Struct Mol Biol*. 2006;13(8):704–712.
32. Shearn A, Rice T, Garen A, Gehring W. Imaginal disc abnormalities in lethal mutants of Drosophila. *Proc Natl Acad Sci U S A*. 1971;68(10):2594–2598.
33. Tripoulas N, LaJeunesse D, Gildea J, Shearn A. The Drosophila ash1 gene product, which is localized at specific sites on polytene chromosomes, contains a SET domain and a PHD finger. *Genetics*. 1996;143(2):913–928.
34. Gregory GD, et al. Mammalian ASH1L is a histone methyltransferase that occupies the transcribed region of active genes. *Mol Cell Biol*. 2007;27(24):8466–8479.
35. Tanaka Y, Kawahashi K, Katagiri Z, Nakayama Y, Mahajan M, Kioussis D. Dual function of histone H3 lysine 36 methyltransferase ASH1 in regulation of Hox gene expression. *PLoS One*. 2011;6(11):e28171.
36. Tanaka Y, Nakayama Y, Taniguchi M, Kioussis D. Regulation of early T cell development by the PHD finger of histone lysine methyltransferase ASH1. *Biochem Biophys Res Commun*. 2008;365(3):589–594.
37. An S, Yeo KJ, Jeon YH, Song JJ. Crystal structure of the human histone methyltransferase ASH1L catalytic domain and its implications for the regulatory mechanism. *J Biol Chem*. 2011;286(10):8369–8374.
38. Yuan W, Xu M, Huang C, Liu N, Chen S, Zhu B. H3K36 methylation antagonizes PRC2-mediated H3K27 methylation. *J Biol Chem*. 2011;286(10):7983–7989.
39. Tanaka Y, Katagiri Z, Kawahashi K, Kioussis D, Kita-

jima S. Trithorax-group protein ASH1 methylates histone H3 lysine 36. *Gene*. 2007;397(1):161–168.
40. Kiel MJ, Yilmaz OH, Iwashita T, Yilmaz OH, Terhorst C, Morrison SJ. SLAM family receptors distinguish hematopoietic stem and progenitor cells and reveal endothelial niches for stem cells. *Cell*. 2005;121(7):1109–1121.
41. Kim I, He S, Yilmaz OH, Kiel MJ, Morrison SJ. Enhanced purification of fetal liver hematopoietic stem cells using SLAM family receptors. *Blood*. 2006;108(2):737–744.
42. Yang L, et al. Identification of Lin(-)Sca1(+)kit(+)CD34(+)Flt3- short-term hematopoietic stem cells capable of rapidly reconstituting and rescuing myeloablated transplant recipients. *Blood*. 2005;105(7):2717–2723.
43. Christensen JL, Weissman IL. Flk-2 is a marker in hematopoietic stem cell differentiation: a simple method to isolate long-term stem cells. *Proc Natl Acad Sci USA*. 2001;98(25):14541–14546.
44. Oguro H, Ding L, Morrison SJ. SLAM family markers resolve functionally distinct subpopulations of hematopoietic stem cells and multipotent progenitors. *Cell Stem Cell*. 2013;13(1):102–116.
45. Weissman IL, Shizuru JA. The origins of the identification and isolation of hematopoietic stem cells, and their capability to induce donor-specific transplantation tolerance and treat autoimmune diseases. *Blood*. 2008;112(9):3543–3553.
46. Rossi L, et al. Less is more: unveiling the functional core of hematopoietic stem cells through knockout mice. *Cell Stem Cell*. 2012;11(3):302–317.
47. Matsumoto A, et al. p57 is required for quiescence and maintenance of adult hematopoietic stem cells. *Cell Stem Cell*. 2011;9(3):262–271.
48. Milne TA, et al. Menin and MLL cooperatively regulate expression of cyclin-dependent kinase inhibitors. *Proc Natl Acad Sci U S A*. 2005;102(3):749–754.
49. Milne TA, Dou Y, Martin ME, Brock HW, Roeder RG, Hess JL. MLL associates specifically with a subset of transcriptionally active target genes. *Proc Natl Acad Sci U S A*. 2005;102(41):14765–14770.
50. Artinger EL, et al. An MLL-dependent network sustains hematopoiesis. *Proc Natl Acad Sci U S A*. 2013;110(29):12000–12005.
51. Cancelas JA, Lee AW, Prabhakar R, Stringer KF, Zheng Y, Williams DA. Rac GTPases differentially integrate signals regulating hematopoietic stem cell localization. *Nat Med*. 2005;11(8):886–891.
52. Trowbridge JJ, Snow JW, Kim J, Orkin SH. DNA methyltransferase 1 is essential for and uniquely regulates hematopoietic stem and progenitor cells. *Cell Stem Cell*. 2009;5(4):442–449.
53. Yokoyama A, Somervaille TC, Smith KS, Rozenblatt-Rosen O, Meyerson M, Cleary ML. The menin tumor suppressor protein is an essential oncogenic cofactor for MLL-associated leukemogenesis. *Cell*. 2005;123(2):207–218.
54. Maillard I, et al. Menin regulates the function of hematopoietic stem cells and lymphoid progenitors. *Blood*. 2009;113(8):1661–1669.
55. Chen YX, et al. The tumor suppressor menin regulates hematopoiesis and myeloid transformation by influencing Hox gene expression. *Proc Natl Acad Sci U S A*. 2006;103(4):1018–1023.
56. Yoshihara H, et al. Thrombopoietin/MPL signaling regulates hematopoietic stem cell quiescence and interaction with the osteoblastic niche. *Cell Stem Cell*. 2007;1(6):685–697.
57. Yamazaki S, Iwama A, Takayanagi S, Eto K, Ema H, Nakauchi H. TGF-beta as a candidate bone marrow niche signal to induce hematopoietic stem cell hibernation. *Blood*. 2009;113(6):1250–1256.
58. Lawrence HJ, et al. Loss of expression of the Hoxa-9 homeobox gene impairs the proliferation and repopulating ability of hematopoietic stem cells. *Blood*. 2005;106(12):3988–3994.
59. Di-Poi N, Koch U, Radtke F, Duboule D. Additive and global functions of HoxA cluster genes in mesoderm derivatives. *Dev Biol*. 2010;341(2):488–498.
60. Martins VC, et al. Thymus-autonomous T cell development in the absence of progenitor import. *J Exp Med*. 2012;209(8):1409–1417.
61. Peaudecerf L, et al. Thymocytes may persist and differentiate without any input from bone marrow progenitors. *J Exp Med*. 2012;209(8):1401–1408.
62. Sun J, et al. Clonal dynamics of native haematopoiesis. *Nature*. 2014;514(7522):322–327.
63. Wang Z, Li G, Tse W, Bunting KD. Conditional deletion of STAT5 in adult mouse hematopoietic stem cells causes loss of quiescence and permits efficient nonablative stem cell replacement. *Blood*. 2009;113(20):4856–4865.
64. Schaefer BC, Schaefer ML, Kappler JW, Marrack P, Kedl RM. Observation of antigen-dependent $CD8^+$ T-cell/ dendritic cell interactions in vivo. *Cell Immunol*. 2001;214(2):110–122.
65. Crabtree JS, et al. Of mice and MEN1: Insulinomas in a conditional mouse knockout. *Mol Cell Biol*. 2003;23(17):6075–6085.
66. Kuhn R, Schwenk F, Aguet M, Rajewsky K. Inducible gene targeting in mice. *Science*. 1995;269(5229):1427–1429.